Imposition of the essential boundary conditions in transient heat conduction problem based on Isogeometric analysis

S. Shojaee*, E. Izadpanah, S. Nazari

Department of Civil Engineering, Shahid Bahonar University, Kerman, Iran

Abstract

The purpose of this paper is using the proposed two step method to impose essential boundary conditions for improving the accuracy of solution field. In the proposed approach, imposing essential boundary conditions in transient heat flow within two-dimensional region is extended in two steps. The essential boundary conditions are defined on Dirichlet boundary as determined temperatures and independent of time. In the first step, Dirichlet boundary conditions are weakly built into the variational formulation, choosing weight function, appropriately. In the second step, with fixed condition, the system of equations is appropriately adjusted. For investigation of the efficiency of the proposed approach, several 2D numerical examples have been performed. The results demonstrate significant improvement in accuracy and rate of convergence in comparison with direct imposition of essential boundary condition.

Keywords: *Isogeometric analysis, essential boundary condition, transient heat flow, NURBS.*

1. Introduction

Isogeometric analysis (IGA) is a recently developed computational approach that offers the possibility of integrating integrating NURBS-based Computer Aided Design (CAD) tools into the conventional finite element analysis. The concept of the IGA in mechanical problems is pioneered by Hughes and his co-workers as a novel technique for discretization of partial differential equations [1]. The basic idea and the core of IGA are to utilize the basis functions that are able to model geometry exactly, from the CAD points of view, for numerical simulations

*E-mail address of the corresponding author: saeed.shojaee@uk.ac.ir (S. Shojaee)
Fax Number: +98-3413220054, Telephone: +98-3413202559

of physical phenomena. This can be achieved by using the B-splines or Non Uniform Rational B-splines (NURBS) for the geometrical description and invoke the isoparametric concepts to define the unknown field variables. The IGA-based approaches have been constantly developed and shown many great advantages for solving variety of different problems in a wide range of research areas, such as fluid–structure interaction, shells, structural analysis and so on [2-9].

In spite of these advantages, the IGA method suffers from some deficiencies. One of the most significant drawbacks arises from imposition of essential boundary conditions. Due to the non-interpolating nature of NURBS basis functions, the Kronecker Delta properties are not satisfied, and as a consequence, the imposition of essential boundary conditions needs special treatment. In considering this, several methods have been proposed for imposing essential boundary conditions in IGA. This issue for NURBS-based isogeometric analysis was first discussed by Hughes et al. [1]. In their research, the essential boundary conditions were imposed to the control variables by evaluating the function of boundary condition at the spatial locations of the control points. In current study, this approach is referred to as Direct Method (DM), mentioned by Wang and Xuan [10]. This method is efficient for homogenous boundary conditions, but it is not reliable for non-homogenous boundary conditions. In addition, when the position of boundary control points is not located on the desired boundary, it is not even reasonable to enforce the given boundary values to the corresponding boundary control variables [10]. Therefore, the enhancement of essential boundary conditions in IGA needs to be researched more thoroughly [1]. Wang and Xuan [10] have proposed an improved method for imposition of essential boundary conditions in IGA, which is based on concepts of the mixed transformation method that was originated by Chen and Wang [11]. In their work, instead of evaluating function of boundary on special location of control points, boundary value of control points were calculated by interpolation on Dirichlet boundary. This method produces more accurate results and convergence rates in comparison with DM [10]. Although Wang and Xuan [11] mentioned that a set of boundary interpolation points can be selected to construct the appropriate transformation matrix it should be considered that selected boundary points can result in singular transformation matrix[12].

Imposing essential boundary conditions in time dependent problems is applied in IGA with Hughes et. al. [5]. They applied direct method in structural vibrations and wave propagation

problems. As mentioned above, DM is able to impose homogenous essential boundary conditions accurately. Bazilevs and Hughes [13] weakly enforced Dirichlet boundary conditions and compared with strongly enforced conditions for boundary layer solutions of the advection–diffusion equation and incompressible Navier–Stokes equations. In their proposed method, they developed stabilized formulations, incorporating weak enforcement of Dirichlet boundary conditions. They also applied this method in computation of flows about rotating components [2]. Cottrell et. al. [7] applied direct method in structural vibrations and learned that inhomogeneous boundary condition and the boundary values must be approximated by functions lying within the NURBS space. This resulted in strong, but approximated satisfaction of the boundary conditions.

In this paper, imposing essential boundary conditions in transient heat flow within two-dimensional region is extended in two steps. The essential boundary conditions are defined on Dirichlet boundary as determined temperatures and independent of time. In the first step, Dirichlet boundary conditions are weakly built into the variational formulation, choosing weight function, appropriately. In the second step, with fixed condition, the system of equations is appropriately adjusted.

This paper is organized as follows: First, the NURBS-based IGA is briefly reviewed. Then, the framework of isogeometric analysis, dealing with transient heat conduction is discussed. Two steps of proposed approach used in transient heat conduction are described and the formulation of such process is presented. Subsequently, several numerical simulations are illustrated to demonstrate the robustness and efficacy of the present method.

2. Isogeometric analysis based on the NURBS basis functions

The traditional finite element formulations are based on interpolation schemes with Lagrange or Hermit polynomials to approximate the geometry, the physical field and its derivatives. This approach often requires a substantial simplification of the geometry, particularly in the case of curved boundaries of the analysis domain. Generally, adaptive refinement of the discretized domain is applied to better approximate the boundary and to achieve sufficient convergence. The concept of IGA is based on applying the NURBS basis functions in accurate modeling of

geometry and approximation of solution space. The NURBS basis functions are weighted functions which originate from B-spline interpolation. The B-spline functions are generated from a knot vector, which is a non-decreasing sequence of coordinates in the parameter space written as,

$$\xi = \left\{ \xi_1, \xi_2, ..., \xi_{n+p+1} \right\} , \tag{1}$$

where ξ_i is the i[th] knot value, *n* and *p* are the number and the order of basis functions defined on knot vector, respectively. The half open interval, $[\xi_i, \xi_{i+1})$, is called knot interval. If $\xi_i = \xi_{i+1}$, then the length of knot interval is equal to zero. If ξ_1 and ξ_{n+p+1} are repeated *p*+1 times in a knot vector, the resulting knot vector is called open knot vector. B-spline basis functions are starting from piecewise constants

$$N_{i,0}(\xi) = \begin{cases} 1 & \text{if } \xi_i \le \xi < \xi_{i+1} \\ 0 & \text{otherwise} \end{cases} \tag{2}$$

and arbitrary polynomial degree *j* can be generated recursively with

$$\begin{aligned} & N_{i,j}(\xi) = \frac{\xi - \xi_i}{\xi_{i+j} - \xi_i} N_{i,j-1}(\xi) + \frac{\xi_{i+j+1} - \xi}{\xi_{i+j+1} - \xi_{i+1}} N_{i+1,j-1}(\xi) \\ & j = 1, 2...., p \\ & i = 1, 2, ..., n + p + 1 - j \end{aligned} \tag{3}$$

in which $N_{i,j}$ is the i^{th} basis function with a *j* order. The first order derivative of B-spline is

$$\frac{d}{d\xi} N_{i,j}(\xi) = \frac{j}{\xi_{i+j} - \xi_i} N_{i,j-1}(\xi) - \frac{j}{\xi_{i+j+1} - \xi_{i+1}} N_{i+1,j-1}(\xi) \ . \tag{4}$$

The B-spline basis functions which are constructed from the open knot vectors have the interpolation feature at the ends of the parametric space. A cubic B-spline basis functions with the interpolation feature at the ends of the parametric space are shown in Fig. 1.

The NURBS basis functions are made from B-spline functions by following equation:

$$R_{i,p}(\xi) = \frac{N_{i,p} w_i}{W(\xi)} \ , \tag{5}$$

in which w_i is the weight corresponding to i^{th} control point and $W(\xi)$ is the weight function as defined by:

$$W(\xi) = \sum_{i=1}^{n} N_{i,p} w_i \ . \tag{6}$$

The bivariate NURBS functions on $\xi - \eta$ knot surface are defined by:

$$R_{i,j}^{p,q}(\xi,\eta) = \frac{N_{i,p}(\xi) M_{j,q}(\eta) w_{i,j}}{W(\xi,\eta)} \ , \tag{7}$$

$i = 1, 2...., n$

$j = 1, 2..., m$

in which $M_{j,q}$ and $N_{i,p}(\xi)$ are respectively the i^{th} p-order and j^{th} q-order functions on ξ and η knot vectors. $w_{i,j}$ is the weight corresponding to ij control point and $W(\xi,\eta)$ is the bivariate weight function, which is given by:

$$W(\xi,\eta) = \sum_{i=1}^{n} \sum_{j=1}^{m} N_{i,p}(\xi) M_{j,q}(\eta) w_{i,j} \ . \tag{8}$$

2.1. *knot insertion*

Simple and straightforward refinement is one of the great advantages of IGA in comparison to classical finite element method. It is very straightforward for increasing number of elements and elevating degree of NURBS basis functions. In this paper, knot-insertion or h-refinement is employed for convergence study. In each refinement step, knots are added to the knot spans. Knot insertion is a procedure that arbitrary new knots are added to a knot vector without any change in the shape of the B-spline curve. If there are $m = n + p + 1$ knots in the knot vector of the B-spline curve, where n is the number of control points and p is the order of B-spline

curve, by adding a new knot, a new control point must be added. Also, some current control points must be redefined.

Consider a knot vector $\xi = \{\xi_1, \xi_2, ..., \xi_{m=n+p+1}\}$ with n control points $P_1, P_2, ..., P_n$ and the order of p. Let $\hat{\xi} \in [\xi_k, \xi_{k+1}]$ be a desired new knot. The knot insertion procedure has the following 3 steps [14]:

1. Find k such that $\hat{\xi}$ belongs to $[\xi_k, \xi_{k+1}]$.
2. Find $p+1$ control points $P_{k-p}, P_{k-p+1}, ..., P_k$.
3. Compute p new control points Q_i from the above $p+1$ control points by using Eq. (9).

$$Q_i = (1-\alpha_i)P_{i-1} + \alpha_i P_i \ , \tag{9}$$

where α_i is obtained from:

$$\alpha_i = \frac{\hat{\xi} - \xi_i}{\xi_{i+p} - \xi_i} \quad \text{for} \quad k-p+1 \le i \le k \, . \tag{10}$$

By performing the above procedure, the new knot vector and control points are obtained by:

$$\{\xi_1, \xi_2, ..., \xi_k, \hat{\xi}, \xi_{k+1}, ..., \xi_m\} \ , \tag{11}$$

$$\{P_1, P_2, ..., P_{k-p}, Q_{k-p+1}, Q_{k-p+2}, ..., Q_k, P_k, P_{k+1}, ..., P_n\} \, . \tag{12}$$

Now, this knot insertion algorithm is extended to a NURBS curve. For this purpose, a given NURBS curve in d-dimensional space is converted into a B-spline curve in *(d+1)*-dimensional space, then by applying the knot insertion algorithm in this B-spline curve, the new control points are obtained. These new control points should then be projected to d-dimensional space to obtain the new control points of the NURBS curve. Consider control points $P_i = (x_i, y_i)$ with corresponding weights of w_i, by converting these control points to 3-dimensional space, $P_i^w = (w_i x_i, w_i y_i, w_i)$, the new control points are then computed from Eq. (13).

$$Q_i^w = (1-\alpha_i)P_{i-1}^w + \alpha_i P_i^w \, . \tag{13}$$

The location of control points in *2D* are obtained by the following projection technique:

$$Q_i = \frac{(1-\alpha_i)P_{i-1}^w + \alpha_i P_i^w}{(1-\alpha_i)w_{i-1} + \alpha_i w_i}, \tag{14}$$

and the weights are:

$$w_{Q_i} = (1-\alpha_i)w_{i-1} + \alpha_i w_i \ . \tag{15}$$

3. Governing equations and discretization

In this section, the governing and discretized equations for the transient heat conduction are briefly presented.

3.1 Transient Heat Conduction

Consider the time dependent equation governing the transient heat transfer in a homogeneous two dimensional region Ω with total boundary Γ;

$$\frac{\partial u}{\partial t} = c^2 \nabla^2 u \quad , \quad c^2 = \frac{k}{\sigma\rho} \ , \tag{16}$$

with boundary conditions:

$$\begin{cases} u = g \quad on\ \Gamma_D \\ \dfrac{\partial u}{\partial n} = h \quad on\ \Gamma_N \end{cases} \tag{17}$$

Here *k* denotes heat transfer coefficient, σ is the specific heat of the material and ρ is its density (mass per unit volume). As shown in Eq. (17) essential and natural boundary conditions are defined as specified time independent temperature and heat flux, respectively. It is assumed that the boundary Γ of an admissible region Ω can satisfy the following conditions:

$$\begin{aligned} &\Gamma_D \cup \Gamma_N = \partial\Omega \\ &\Gamma_D \cap \Gamma_N = \varnothing \end{aligned} \tag{18}$$

where Γ_D is the admissible Dirichlet boundary and Γ_N is the Neumann boundary. It is assumed that the materials are homogenous and time independent.

3.2 Variational approximation

Several well-established weighted residual methods such as Galerkin method, the method of least square, collocation and subdomain methods can be used to approximate the solution. Here, we consider the Galerkin method to seek an approximate solution to transient heat transfer equation. Assume S and V to be the subspaces of function space with a continuous second derivative;

$$S = \left\{ f \mid f \in H^1(\Omega),\ f|_{\Gamma_D} = g \right\}$$
$$V = \left\{ r \mid r \in H^1(\Omega), r|_{\Gamma_D} = 0 \right\} \tag{19}$$

where $H^1(\Omega)$ is Sobolev space, which can be defined as:

$$H^1(\Omega) = \left\{ u \mid D^\alpha u \in L^2(\Omega), |\alpha| \le 1 \right\}. \tag{20}$$

The semi discrete weak variational formulation of Eq. (16) over Ω is given by

$$\int w \frac{\partial u}{\partial t}\, d\Omega = c^2 \left[\int_{\Gamma_N} wh\, d\Gamma - \int_\Omega \nabla w . \nabla u\, d\Omega \right]. \tag{21}$$

The main difference between the proposed method and the other methods is, how to choose *W* (i.e. weight function). In the conventional method, weight function is considered from *V*, but in the proposed two-step method, it is considered from *S* space. In this subsection, the conventional method is discussed, initially. Considering $u = v + g$ and $\frac{\partial u}{\partial t} \approx \frac{\Delta u}{\Delta t}$, and substitute in Eq. (21)

$$\int_\Omega w\, \Delta v\, d\Omega + \int_\Omega w\, \Delta g\, d\Omega = c^2 \Delta t \left[\int_{\Gamma_N} wh\, d\Gamma - \int_\Omega \nabla w . \nabla v\, d\Omega - \int_\Omega \nabla w . \nabla g\, d\Omega \right], \tag{22}$$

where g is prescribed temperature on Γ_D and v belong to *V*. The NURBS approximation of v , g , Δv , Δf_b and w are given by

$$v \approx R_i \bar{v} \tag{23a}$$
$$g \approx R_b \bar{g} \tag{23b}$$
$$\Delta v \approx R_i d_i \tag{23c}$$
$$\Delta g \approx R_b d_b \tag{23d}$$
$$w \approx R_i \bar{w} \tag{23e}$$

where R_i and R_b are interior and boundary basis function matrices, respectively (see [10, 12] for more details); $\bar{v}$ and $\bar{g}$ are vector of interior and boundary control points temperature respectively. d_i and d_b are vector of interior and boundary control points temperature gradient. $\bar{w}$ is the weight vector of interior control points. Δt is time interval. The temperature is assumed to be constant by the time on Γ_D that means $\Delta g = d_b = 0$. The matrix form of equations can be obtained by substituting Eqs. (23) to Eq. (22):

$$K d_i^{n+1} = F_N + F_D + F_\Omega^n \ , \tag{24}$$

and,

$$K = \int_\Omega R_i^T . R_i \ d\Omega \tag{25a}$$

$$F_N = c^2 \Delta t \int_{\Gamma_N} R_i^T \ h \ d\Omega \tag{25b}$$

$$F_D = -c^2 \Delta t \int_\Omega \nabla R_i^T . \nabla R_b \ d\Omega \ \bar{g} \tag{25c}$$

$$F_\Omega^n = -c^2 \Delta t \int_\Omega \nabla R_i^T . \nabla R_i \ d\Omega \bar{v}^n \tag{25d}$$

where *n* shows the *nth* time interval. We can use two approaches to estimate $\bar{g}$. In the first approach, the temperature of boundary control points is imposed by evaluating the function of boundary condition at the spatial locations of the control points. This method suffers from two essential drawbacks. When the position of boundary control points is not located on the desired boundary and it is not reasonable to enforce the given boundary temperatures to the corresponding boundary control variables. In addition, the non-interpolating nature of NURBS basis functions does not allow for the satisfaction of inhomogeneous boundaries in a straightforward approach, and offers a lower rate of convergence. In the second approach, the vector $\bar{g}$ is obtained by interpolation of function on boundary. It offers a far higher rate of convergence in comparison with the first approach. However, it should be considered that selected boundary points can result in a singular transformation matrix. This drawback is more significant when there are many active control points on the desired boundary, which requires a more precise selection procedure. As mentioned by Wang and Xuan [10], a set of boundary interpolation points can be selected to construct the appropriate transformation matrix.

3.3 Proposed Method

3.3.1 Step1

As discussed earlier, for the conventional methods, since $W \in V$, the integration on Dirichlet boundary becomes zero and the usual weak formulation (15) can be obtained. In the proposed method, the weight function, W belongs to S, and a change in the weight function causes a corresponding change in weak formulation as:

$$\int w\frac{\partial u}{\partial t}\,d\Omega = c^2\left[\int_{\Gamma_N} wh\,d\Gamma + \int_{\Gamma_D} w\frac{\partial u}{\partial n}\,d\Gamma - \int_{\Omega} \nabla w.\nabla u\,d\Omega\right]. \tag{26}$$

The functions w and u are approximated by total NURBS functions,

$$u \approx R\bar{u} \tag{27a}$$

$$w \approx R\bar{w} \tag{27b}$$

where R is the total basis function matrix. Comparing Eq. (27b) and Eq. (23e) shows the main difference between conventional and proposed methods that's the space of w function. In other words if you choose $w \in V$ it leads to strongly imposition of essential boundary condition and on the other hand selecting $w \in S$ leads to weakly imposition of essential boundary condition. The second term on the right side of Eq. (25) is the integration on Dirichlet boundary; where n is the outward unit normal to Dirichlet boundary.

$$\int_{\Gamma_D} w\frac{\partial u}{\partial n}\,d\Gamma = \int_{\Gamma_D} w\begin{bmatrix} n_x & n_y \end{bmatrix}\nabla u\,d\Gamma\,. \tag{28}$$

One of the problems in the proposed method is the characteristic determination of vector n. The vector n is formed by cross product of $\vec{t}$ and $\vec{s}$, where these vectors are perpendicular to the plane of problem and tangent to the surface, respectively.

The correct direction of vector n depends on exact choice of the direction of $\vec{t}$. As shown in Fig. (2), if the given direction of $\vec{t}$ shall be changed, the direction of n is changed. The exact selection of $\vec{t}$ is defined as cross product of vectors $\vec{s}$ and $\vec{m}$. $\vec{m}$ is a vector from boundary to region and defined thorough $\bar{p}_b$ and $\bar{p}_i$ points. $\bar{p}_b$ is a point on Dirichlet boundary and $\bar{p}_i$ is a point in Ω space near to the $\bar{p}_b$.

$$\vec{t} = \vec{s} \times \vec{m} = \begin{bmatrix} \dfrac{\partial x}{\partial l} \\ \dfrac{\partial y}{\partial l} \end{bmatrix} \times (\bar{p}_i - \bar{p}_b), \tag{29}$$

where *l* is the direction of Dirichlet boundary in parametric space (see Fig. (3)).

It is worthwhile to note that, if $\bar{p}_i$ is selected inappropriately incorrect direction of $\vec{t}$ shall be obtained. Two situations may occur;

1. $\bar{p}_i$ may be placed along the $\vec{s}$ vector that results to $\vec{t} = 0$ (see Fig. (4a)).
2. Incorrect placement of $\bar{p}_i$ leads to the incorrect direction of $\vec{t}$ (see Fig. (4b)).

It is clear that the appropriate selection of $\bar{p}_i$ in the physical space is not simple, and therefore, it is selected in the parametric space. Assume that $\hat{p}_b(\xi_b, \eta_b)$ and $\hat{p}_i(\xi_i, \eta_i)$ are images of $\bar{p}_b(x_b, y_b)$ and $\bar{p}_i(x_i, y_i)$ in the parametric space, respectively. The appropriate placement of $\bar{p}_i$, $\hat{p}_i(\xi_i, \eta_i)$ is selected as follow:

$$\begin{aligned} &f\ l = \xi \ \rightarrow\ \xi_i = \xi_b\ ,\ \eta_i = \eta_b \pm \alpha L_\eta \\ &f\ l = \eta \ \rightarrow\ \eta_i = \eta_b\ ,\ \xi_i = \xi_b \pm \alpha L_\xi \end{aligned} \tag{30}$$

where L_ξ and L_η are the lengths of parametric space in ξ and η directions. Parameter α is a constant that belongs to (0,1]. Finally, the vector *n* can be obtained by:

$$n = y_l(x_l y_{ib} - y_l x_{ib})\vec{i} - x_l(x_l y_{ib} - y_l x_{ib})\vec{j}\ , \tag{31}$$

Where $(\,)_l$ denotes $\dfrac{\partial(\,)}{\partial l}$ and $()_{ib}$ denotes $(\,)_i - (\,)_b$. Accordingly, the variational statement of Eq. (25) leads to the matrix form as;

$$Kd^{n+1} = F_N + F_D^n + F_\Omega^n\ , \tag{32}$$

where matrix *K*, vectors F_N and F_Ω^n are defined in Eq. (24). The evaluation of these parameters can be performed using the complete NURBS basis functions. The vector F_D^n is defined as:

$$F_D^n = c^2 \Delta t \int_{\Gamma_D} \tilde{R}^T \times \nabla R \, d\Gamma \, \bar{u}^n\ . \tag{33}$$

Here, R is the matrix of the NURBS basic functions and $\bar{u}^n$ is the control points temperature vector in n^{th} time step, and $\tilde{R}$ is defined as:

$$\tilde{R} = (x_l y_{ib} - y_l x_{ib}) \begin{bmatrix} y_l \\ -x_l \end{bmatrix} R . \tag{34}$$

Δt is the time step size and should be sufficiently small to achieve the numerical stability, due to the Courant–Friedrichs–Lewy (CFL) condition.

3.3.2 Step2

As discussed above in this paper the essential boundary conditions are imposed in 2 step. In previous subsection first step is described, and in this subsection the second step is explained completely. In this paper the essential boundary conditions are time independent. So, we must modify the system of equations to enforce this condition. According to Eq. (24) it can be done if the temperature variation of boundary control points is equal to zero.

3.4 Initial Condition

Solving the transient heat transfer needs to see how the temperature change from the initial state (i.e. t = 0) to the final steady state as a function of time. In finite element method, the initial temperature at each node is equal to temperature distribution function at node. But in IGA, the non-interpolating nature of NURBS does not allow for determining the initial temperature of control points at the spatial locations. Here, using interpolation inside the physical region, the initial temperature of control points is evaluated.

Assume $H(\Omega)$ to be the initial temperature function and m be the number of NURBS functions on domain. Appropriate choice of m interpolation points leads to the initial temperature of control points, which is given by:

$$\begin{aligned} & T\,\bar{u}^0 = \bar{H} \\ & T_{ij} = R_j(\xi_i, \eta_i) \\ & \bar{H}_i = H(x_i, y_i) \end{aligned} \tag{35}$$

where (ξ_i, η_i) is ith interpolation point in the parametric space and (x_i, y_i) is the projection of this point in the physical space. A set of interpolation points can be selected to construct the solution. Appropriate selection procedure is required to prevent singularity in transformation matrix. For appropriate placement, a set of interpolation points in the maximum points of NURBS functions can be selected.

4. Numerical examples

In this section, the accuracy and the convergence of the proposed method through several numerical examples is verified. The results obtained by the proposed method are also compared with direct and finite element methods. Third order NURBS is used in all examples. For numerical integration 3×3 gauss quadrature rule is applied in the domain and 5 gauss quadrature rule on the boundaries. The material is aluminum, *k* (heat transfer coefficient), σ (the specific heat of the material) and ρ (density or mass per unit volume) are considered, $\rho = 2.7^{(\frac{g}{cm^3})}$, $\sigma = 0.9^{(\frac{J}{g.K})}$, $k = 2.37^{(\frac{J}{cm.s.K})}$

4.1 heat conduction in annulus disk

In this example, the heat conduction in annulus disk is modeled. Geometry and boundary conditions are shown in Figure 5.

As shown in Figure 5, heat transfer is prevented between disk boundaries and other domains, and $\Gamma_D = \varnothing$ is assumed. The initial temperature in entire domain as shown in Figure 6 is considered as:

$$H(\Omega) = 50x^2. \tag{36}$$

$H(\Omega)$ is used to approximate the function $\tilde{H}(\Omega)$ and this is obtained by calculating initial temperature in the control points. Figure 7 illustrates the percentages of the error distribution for $\tilde{H}(\Omega)$. For the convergence study, the h-refinement strategy is employed and meshes with 60, 200, 240 and 360 (Figure 8) elements in IGA and 52, 172, 503 and 1008 in FEM are investigated (see Table 1).

As shown in Figure 9(a), the two-step and direct methods have similar convergence rate, where no essential boundary conditions are defined. In other words, when there are no essential boundary conditions, the direct and proposed methods have the same accuracy. Further, it is shown that, the convergence rate of the proposed and direct methods is better than the classic finite element method. The difference between the results of each step and the result of final step is shown in Figure 9(b) The parameter δ is defined as: $\delta_i = \left|\frac{T_i - T_4}{T_4}\right| \times 100$, for i=1 to 4. It is clear that the proposed and direct methods converge faster than FEM:

Temperature distribution at t=3sec and temperature variation within time at $p = (1.5, 0)$ are shown in Figures 10 and 11, respectively.

4.2 heat conduction on square plate with circular hole

The next example refers to a situation that the initial temperature is defined by multi functions. Here, the multi patch technique is used to divide a square plate into four patches, having a hole in the center as shown in Figure 12. A particular initial temperature is considered for each patch are listed in Table 2.

The outer boundary of the plate is insulated. The essential boundary conditions are defined on boundary of hole as a specified and time-independent temperature. Figure 13(a) shows the initial temperature distribution on domain.

Figure 13(b) confirms that approximated initial temperature is very close to exact one. Similar to the pervious example, the convergence study is carried out increasing the number of elements and cells listed in Table 3 in four steps.

The final meshing includes 720 elements with 880 degree of freedom in IGA (see Figure 14), and 4913 elements with 5131 degree of freedom in FEM.

As shown in Figure 15(a), the two-step and finite element methods converge to the same temperature. However, the result of the direct method in the final meshing is a little different. The reason is essential boundary conditions. Since the function on Dirichlet boundary is not constant or linear, imposing essential boundary conditions through direct method is not accurate.

It also can be found that, in a coarse meshing DM is more accurate than FEM but when the number of elements is increased the result of FEM is more accurate. Figure 15 (b) confirms that the proposed method converge very faster than two other methods. It is clear that the result of two-step method in first step is very close to final step result.

The temperature distribution at t=3sec and temperature variation within time at p= (1.5, 0) are plotted in Figures (16) and (17), respectively:

5. Conclusion

In this paper, a new method is proposed for imposition of the essential boundary conditions in transient heat conduction problem based on isogeometric analysis. This method is named as *two-step method*, because the essential boundary conditions are imposed in two steps. The first step includes calculating the force vector corresponding to the Dirichlet boundaries, and the system of linear equation is modified in the second step. This method is classified in "weakly imposition of the essential boundary condition". The numerical examples confirm that the two-step and the direct methods are similar, when there are no essential boundary conditions. However, in the situation that the essential boundary conditions are more complex, the results for the proposed method offer more accurate solution in comparison with the direct method. Furthermore, comparing the results of the two-step, direct and classic finite element methods, it can be demonstrated that the convergence of the proposed method is faster than two other methods. Also, the numerical examples show that using the two-step method for imposition of the essential boundary conditions enable us to use coarse meshing and obtain a very accurate result.

6. References

1. Hughes, T.J.R., Cottrell, J.A.Y. and Bazilves, Y., "Isogeometric analysis: CAD, finite elements,NURBS, exact geometry and mesh refinement," Comput. Meth. Appl. Mech. Eng., (194), pp 4135–4195 (2005).
2. Bazilevs, Y., Hughes, T.J.R., "NURBS-based isogeometric analysis for the computation of flows about rotating components," Comput. Mech., (43), pp 143–150 (2008).
3. Bazilevs, Y., Michler, C., Calo, V.M., Hughes, T.J.R., "Weak Dirichlet boundary conditions for wall-bounded turbulent flows," Comput. Meth. Appl. Mech. Eng., (196), pp 4853–4862 (2007).
4. Bazilevs, Y., Calo, V.M., Hughes, T.J.R., Zhang, Y.. "Isogeometric fluid–structure interaction: theory, algorithms and computations," Comput. Mech., (43), pp 3–37 (2008).

5. Hughes, T.J.R., Reali, A., Sangalli, G., "Duality and unified analysis of discrete approximations in structural dynamics and wave propagation comparison of p-method finite elements with k-method NURBS," Comput. Meth. Appl. Mech. Eng., (197), pp 4104–4124 (2008).

6. Zhang, Y.J., Bazilevs, Y., Goswami, S., Bajaj, C.L., Hughes, T.J.R., "Patient-specific vascular NURBS modeling for isogeometric analysis of blood flow," Comput. Meth. Appl. Mech. Eng., (196), pp 2943–2959 (2007).

7. Cottrell, J.A., Reali, A., Bazilevs, Y., Hughes, T.J.R., "Isogeometric analysis of structural vibrations," Comput. Meth. Appl. Mech. Eng., (195), pp 5257–5296 (2006).

8. Benson, D.J, Bazilevs, Y., Hsu, M.C., Hughes, T.J.R., "Isogeometric shell analysis: the Reissner–Mindlin shell," Comput. Meth. Appl. Mech. Eng., (199), pp 276–289 (2010).

9. Gómez, H., Calo, V.M., Bazilevs, Y., Hughes, T.J.R., "Isogeometric analysis of the Cahn–Hilliard phase-field model," Comput. Meth. Appl. Mech. Eng., (197), pp 4333–4352 (2008).

10. Wang, D. and Xuan, J., "An improved NURBS-based isogeometric analysis with enhanced treatment of essential boundary conditions," Comput. Meth. Appl. Mech. Eng., (199), pp 2425-2436 (2010).

11. Chen, J.S., Wang, H.P., "New boundary condition treatments in meshless computation of contact problems," Comput. Meth. Appl. Mech. Eng., (187), pp 441–468 (2000).

12. Shojaee, S., Izadpanah, E., and Haeri, A., "imposition of essential boundary conditions in isogeometric analysis using Lagrange multiplier method" International Journal of Optimization in Civil Engineering, (2), pp 247-271, (2012).

13. Bazilevs, Y., Hughes, T.J.R., "weak imposition of dirichlet boundary conditions in fluid mechanics," computer&fluids, (36), pp 12-26 (2007).

14. Piegl L, Tiller W. The NURBS Book (Monographs in visual communication), 2nd ed. Springer. New York, (1997).

Saeed Shojaee obtained his B.S. degree from Shahid Bahonar University of Kerman in 2001, and his M.S. and Ph.D. degrees in Structural Engineering from Iran University of Science and Technology in 2003 and 2007, respectively. He is currently Associate Professor in the Department of Civil Engineering at Shahid Bahonar University in Kerman, Iran. His main research interests include: optimal analysis and design of structures, metaheuristic optimization techniques and applications, computational mechanics and seismic design of structures.

Ebrahim Izadpanah received his M.E. degree in Structural Engineering from the Shahid Bahonar University of Kerman in 2012. He is currently a Ph.D. degree candidate in Shahid Bahonar University of Kerman. His research interests include: computational mechanics and Isogeometric analysis.He has published a number of papers in journals.

Saeed Nazari obtained his B.S. degree from Shahid Bahonar University of Kerman in 2012. He is currently a M. SC. student in Amirkabir University of Technology.

Figures Caption

Figure 1. Cubic basis functions for an open knot vector $\Xi = \{0,0,0,0,0.25,0.5,0.75,1,1,1,1\}$

Figure 2. Outward unit normal vector on Dirichlet boundary, (a) correct direction of n, (b) incorrect direction of n

Figure 3. Direction of Dirichlet boundaries in parametric space

Figure 4. Incorrect placements of $\overline{p}_i$

Figure 5. Geometry and boundary conditions of Annulus disk $\frac{\partial u}{\partial n} = 0 \quad on\ \Gamma_{N1}\ and\ \Gamma_{N2}$

Figure 6. Temperature distribution on annulus disk at t=0

Figure 7. Error distribution of approximated temperature at t=0

Figure 8. Final mesh of annulus disk problem with 360 elements in IGA

Figure 9. Convergence procedure of two-step, direct and finite element methods for annulus disk problem

Figure 10. Temperature distribution on disk at t=3sec

Figure 11.Temperature variation within time at p= (1.5, 0)

Figure 12. Square plate with circular hole in center

Figure 13. (a) Temperature distribution on square plate with circular hole at t=0,

(b) Error distribution of approximated temperature at t=0

Figure 14. Final meshing of example 2 with 720 elements in IGA

Figure 15. Convergence procedure of two-step, direct and finite element methods for example 2
(a) Absolute temperature, (b) Relative temperature with respect to final meshing

Figure 16. Temperature distribution on annulus disk at t=3sec

Figure 17. Temperature variation within time at p= (1.5, 0)

Tables Caption

Table 1. Refinement procedure of annulus disk problem in IGA and FEM

Table 2. Initial temperature and boundary conditions in each patch

Table 3. Refinement procedure of square plate problem in IGA and FEM

Figure 1. Cubic basis functions for an open knot vector $\Xi = \{0,0,0,0,0.25,0.5,0.75,1,1,1,1\}$

Figure 2. Outward unit normal vector on Dirichlet boundary, (a) correct direction of n, (b) incorrect direction of n

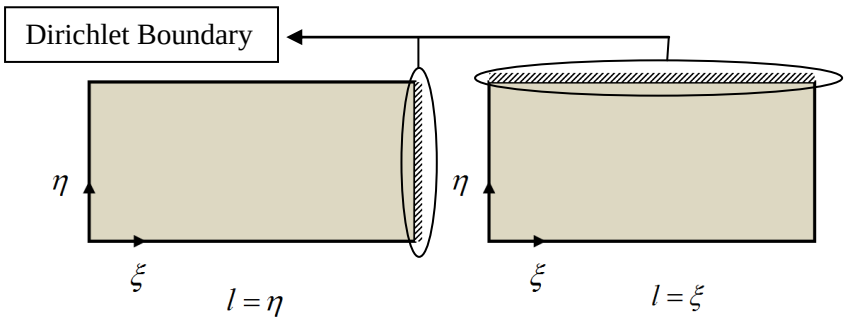

Figure 3. Direction of Dirichlet boundaries in parametric space

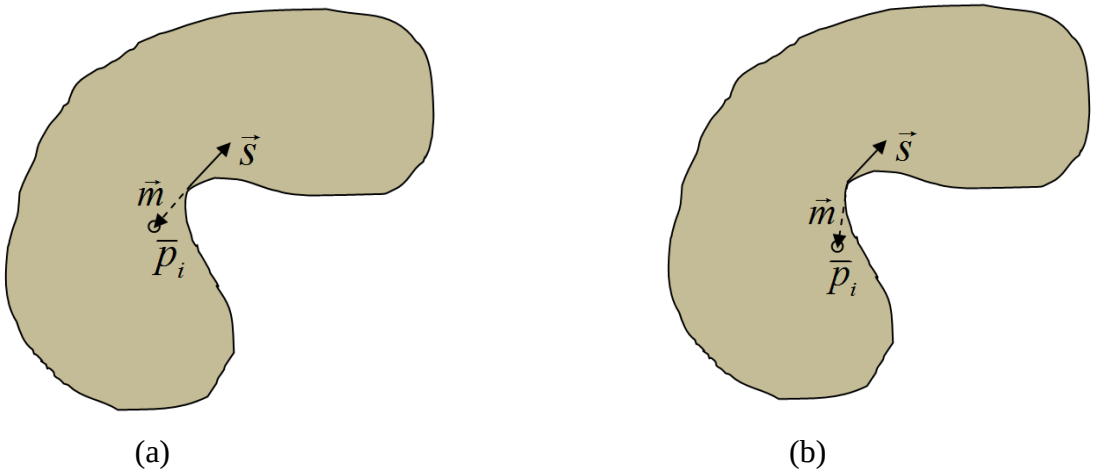

(a) (b)

Figure 4. Incorrect placements of $\overline{p}_i$

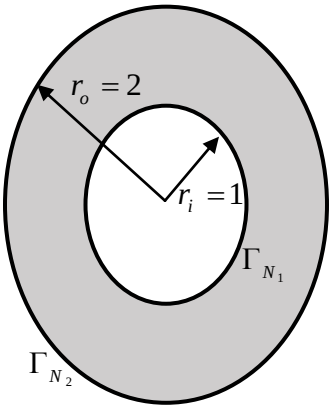

Figure 5. Geometry and boundary conditions of Annulus disk $\frac{\partial u}{\partial n} = 0 \quad on\ \Gamma_{N1}\ and\ \Gamma_{N2}$

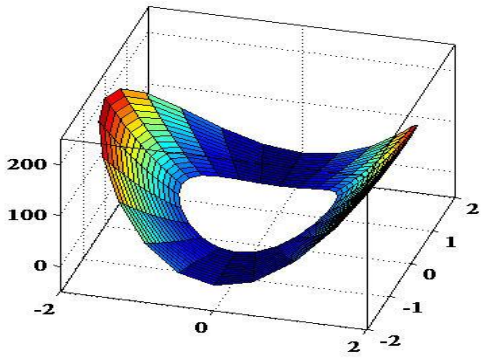

Figure 6. Temperature distribution on annulus disk at t=0

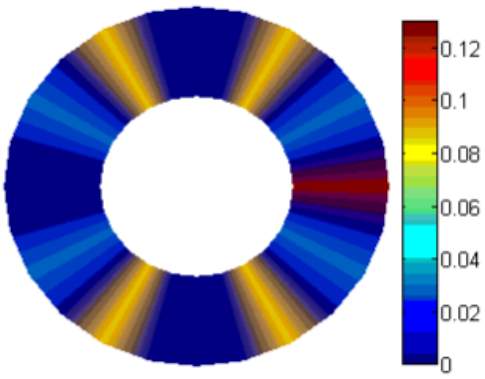

Figure 7. Error distribution of approximated temperature at t=0

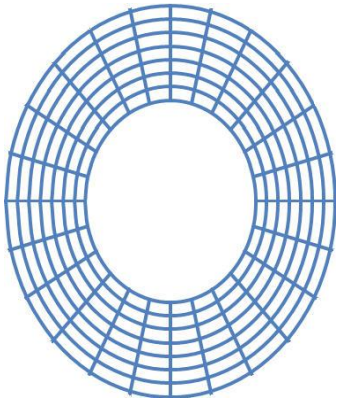

Figure 8. Final mesh of annulus disk problem with 360 elements in IGA

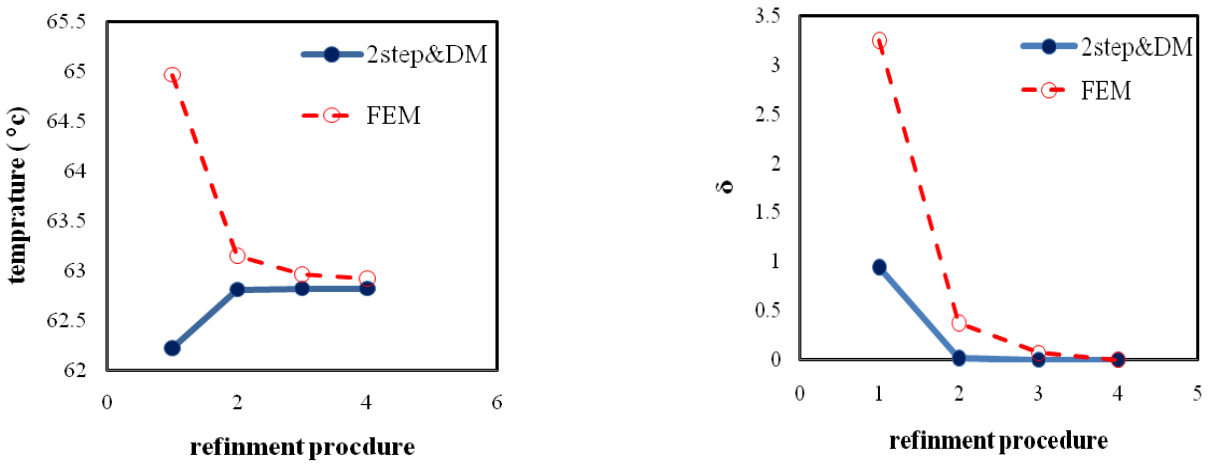

Figure 9. Convergence procedure of two-step, direct and finite element methods for annulus disk problem:

(a) Absolute temperature, (b) Relative temperature with respect to final meshing

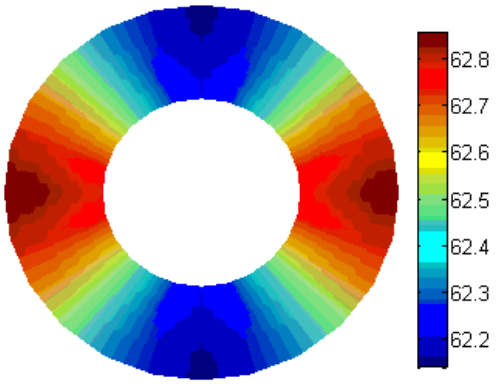

Figure 10. Temperature distribution on disk at t=3sec

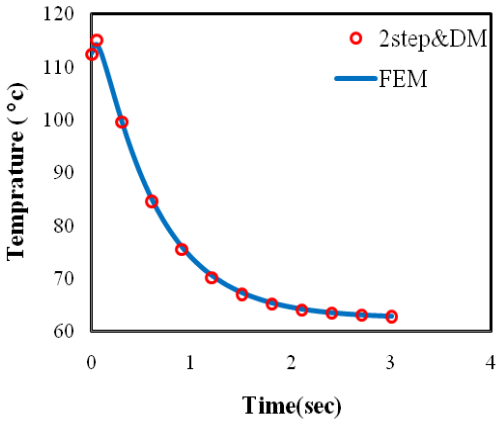

Figure 11.Temperature variation within time at p= (1.5, 0)

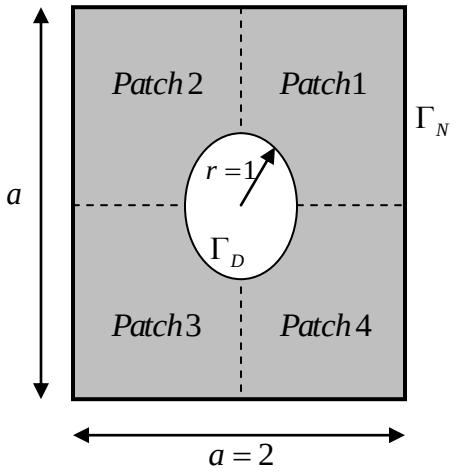

Figure 12. Square plate with circular hole in center

.

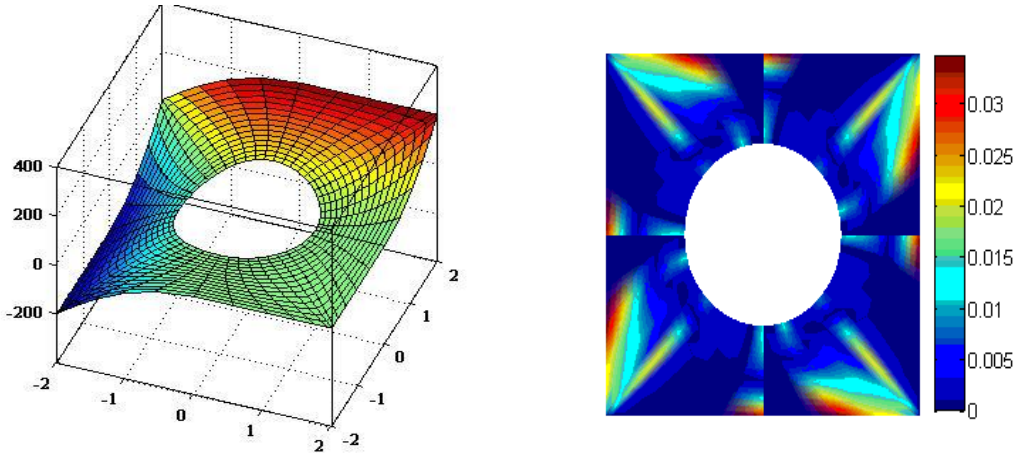

(a) **(b)**

Figure 13. (a) Temperature distribution on square plate with circular hole at t=0,

(b) Error distribution of approximated temperature at t=0

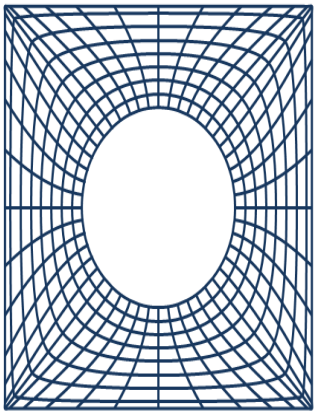

Figure 14. Final meshing of example 2 with 720 elements in IGA

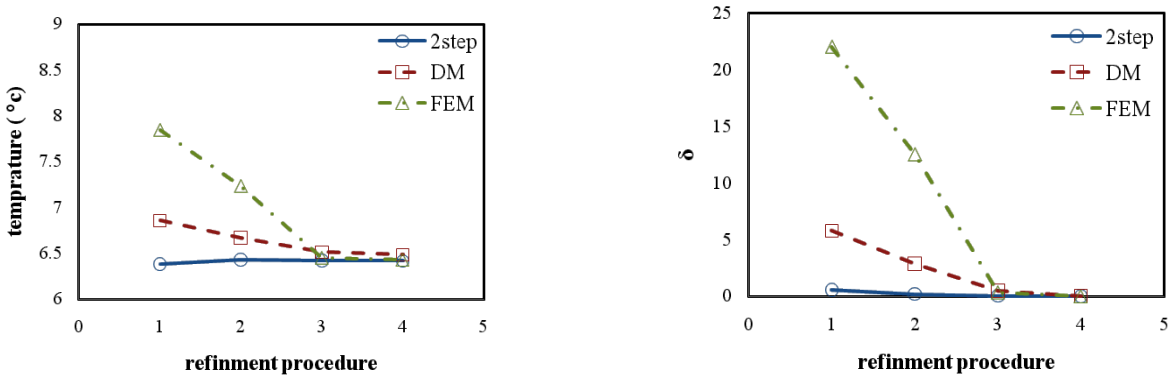

(a) **(b)**

Figure 15. Convergence procedure of two-step, direct and finite element methods for example 2
(a) Absolute temperature, (b) Relative temperature with respect to final meshing

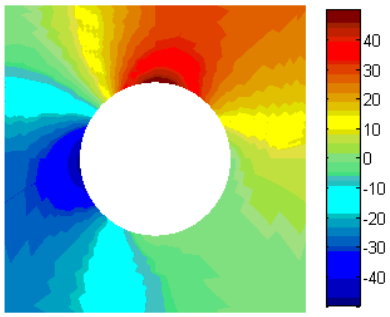

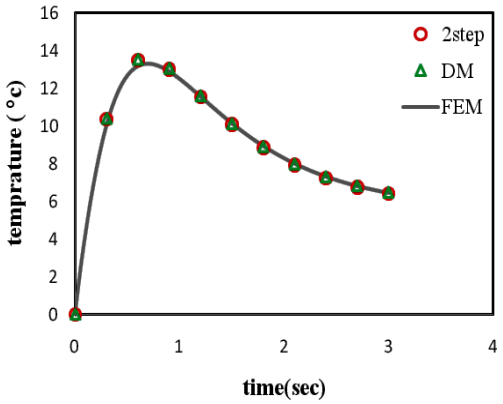

Figure 16. Temperature distribution on annulus disk at t=3sec **Figure 17. Temperature variation within time at p= (1.5, 0)**

Table 1. Refinement procedure of annulus disk problem in IGA and FEM

	Number of elements			
IGA	60	200	240	360
FEM	52	172	503	1008

Table 2. Initial temperature and boundary conditions in each patch:

	Initial temperature	Essential B.C	Natural B.C
Patch1	$H(\Omega) = 50y^2$	$g_1 = 50y^2$	$h_1 = 0$

Patch2	$H(\Omega) = 50(y^2 - x^2)$	$g_2 = 50(y^2 - x^2)$	$h_2 = 0$
Patch3	$H(\Omega) = -50x^2$	$g_3 = -50x^2$	$h_3 = 0$
Patch4	$H(\Omega) = 0$	$g_4 = 0$	$h_4 = 0$

Table 3. Refinement procedure of square plate problem in IGA and FEM

	Number of elements			
IGA	64	120	400	720
FEM	100	657	1258	4913